UNIVERSITY OF WEST BOHEMIA

Applied and Computational Mechanics 1 (2007) 243 - 254

Applied and Computational Mechanics

Modeling wave dispersion and band gaps in heterogeneous elastic media

E. Rohan[a,b,*], F. Seifrt[a]

[a] *Dept. of Mechanics, Faculty of Applied Sciences, UWB in Pilsen, Univerzitní 22, 306 14 Plzeň, Czech Republic*
[b] *New Technologies Research Centre, UWB in Pilsen, Univerzitní 22, 306 14 Plzeň, Czech Republic*

Received 10 September 2007; received in revised form 4 October 2007

Abstract

In this paper we report recent developments and results concerning validation of the homogenization approach applied in modeling waves in strongly heterogeneous elastic media. The homogenization limit model is obtained for stationary waves, but can also be used to estimate dispersion properties for long guided waves propagation. Band gaps distribution depends on the material contrast and on the geometrical arrangements in the microstructure. Similarity between discrete structures and heterogeneous continua is used to demonstrate the dispersion phenomena. The modeling approach has been extended to the piezo-phononic materials, which may be useful in designing smart materials. Also problems of optimal shape design at the microscopic level were pursued.

Keywords: phononic materials, periodic microstructure, homogenization, dispersion, guided waves

1. Introduction

Heterogeneous media with periodic structure gained growing attention in engineering community due to vast applications in design of smart materials. In the context of wave propagation, the *photonic crystals* form important parts of devices for controlling electromagnetic wave propagation, cf. [10, 4]. In analogy, the acoustic waves can be handled using the *phononic crystals* constituted by elastic materials with large difference in their material parameters; modeling this type of media was developed in the framework of the Bloch wave description. Recently in [2, 3] an alternative approach based on the two-scale homogenization theory was presented.

The homogenized model reported here was obtained by asymptotic analysis in the framework of the unfolding method [5] applied to the *strongly heterogeneous medium*; it is characterized by scale-dependent elasticity in one of the composite constituents. The aim of this paper is twofold: firstly, using a simple model of discrete mass-spring periodic structure, to provide an asymptotic analysis illustration of the dispersion phenomenon, as represented by the *band gaps* which result from the stiffness scaling; secondly, having in mind modeling of real composite materials, to study the effect of the material contrast and the microscale size parameter (the scale) on the *modeling approximation* for the case of long guided wave propagation.

2. Dispersion in strongly heterogeneous mass-spring structures

Discrete mechanical structures of the mass-spring type are convenient to demonstrate dispersion properties of structures with large heterogeneity in material coefficients. Here we illustrate

*Corresponding author. Tel.: +420 377 632 320, e-mail: rohan@kme.zcu.cz.

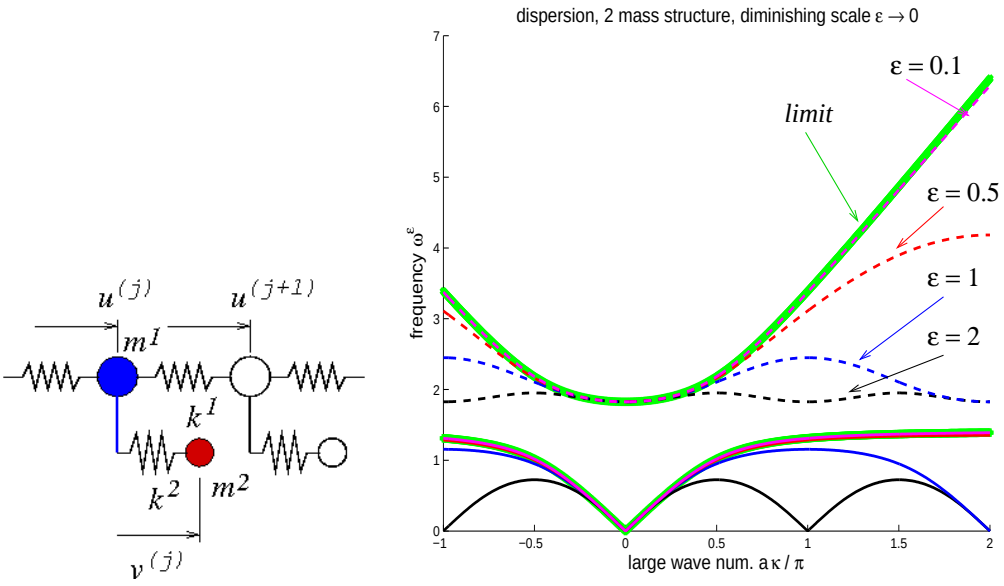

(a) (b)

Fig. 1. (a): the scheme of the model. (b): Dispersion curves (lower and upper branches) for the modified scaling ε (long waves). Horizontal axis: fixed range of wave numbers for all ε considered. Different colors correspond to different scales: $\varepsilon = 2$ ... black, $\varepsilon = 0.1$ ... magenta. The limit dispersion branches displayed in green.

how the dispersion phenomenon depends on the scaling of structural parameters.

2.1. Simple homogeneous chain with small branches

We consider a simple mass-spring 1D structure according to fig. 1a which is formed as a single chain consisting of concentrated masses m_1 connected by springs k_1. Another masses m_2 are attached to each mass m_1 by a spring k_2. We consider wave propagated in the chain, such that its j-th mass undergoes motion $u^{(j)}$

$$\begin{aligned} fig - bgu(t, x^{(j)}) = u^{(j)} = U \exp\{\mathrm{i}(\omega t + ja\kappa)\} \ , \quad j = 1, 2, \ldots , \\ u^{(j+1)} = u^{(j)} \exp\{\mathrm{i}a\kappa\} \ , \\ u^{(j-1)} = u^{(j)} \exp\{-\mathrm{i}a\kappa\} \ , \end{aligned} \tag{1}$$

where a is the distance between two consecutive masses of the chain, $x^{(j)} = ja$ is the geometrical position, κ is the wave number, ω is the frequency. The momentum equations written for both parts of the structure (the chain and the branches) yield

$$\begin{aligned} -\omega^2 m_1 u^{(j)} + k_1(u^{(j)} - u^{(j-1)}) - k_1(u^{(j+1)} - u^{(j)}) - k_2(v^{(j)} - u^{(j)}) = f_1^{(j)} \ , \\ -\omega^2 m_2 v^{(j)} + k_2(v^{(j)} - u^{(j)}) = f_2^{(j)} \ , \end{aligned} \tag{2}$$

where $v^{(j)}$ is the motion of the attached masses m_2. Eigenfrequency of the superimposed motion (represented by $v^{(j)}$) is

$$\lambda = \frac{k_2}{m_2} \ , \text{ hence } v^{(j)} = \frac{\lambda}{\lambda - \omega^2} u^{(j)} + \frac{f_2^{(j)}}{(\lambda - \omega^2) m_2} \ . \tag{3}$$

This substituted in $(2)_1$ with applied $(1)_{2,3}$ leads to the following equation

$$-\omega^2 M(\omega^2)u^{(j)} + K(\kappa)u^{(j)} = \sum_\alpha f_\alpha^{(j)} - \frac{\omega^2}{\omega^2-\lambda} f_2^{(j)} \tag{4}$$

where

$$M(\omega^2) = m_1 + m_2 - m_2\frac{\omega^2}{\omega^2-\lambda}\ , \quad K(\kappa) = 4k_1\sin^2(\frac{a}{2}\kappa)\ . \tag{5}$$

So, the dispersion relationship $\omega = \omega(\kappa)$ is obtained by solving the bi-quadratic equation

$$m_1\omega^4 - \left[\lambda(m_1+m_2) + 4k_1\sin^2(a\kappa/2)\right]\omega^2 + 4\lambda k_1\sin^2(a\kappa/2) = 0\ . \tag{6}$$

2.1.1. Scaling of the structural parameters

We shall now consider a sequence of models characterized by different length scales $\varepsilon \to 0_+$, so that the characteristic length of the microstructure is $a^\varepsilon = \varepsilon\bar{a}$. As the consequence, the actual masses and spring stiffnesses are related to scale parameter ε as follows

$$a^\varepsilon = \varepsilon\bar{a} \ \Rightarrow \quad k_\alpha^\varepsilon = \varepsilon^{-1}\bar{k}_\alpha\ , \qquad m_\alpha^\varepsilon = \varepsilon\bar{m}_\alpha\ , \quad \alpha = 1,2\ . \tag{7}$$

Also we consider magnitudes of the applied forces proportional to masses, thus $f_\alpha^\varepsilon = \varepsilon\bar{f}_\alpha$. However, in order to evoke the *strongly heterogeneous properties* we shall modify the scale dependent stiffness $k_2^\varepsilon := \varepsilon^2\varepsilon^{-1}\bar{k}_2$, so that the eigenfrequency $\lambda^\varepsilon = \bar{\lambda}$ is independent of ε, i.e.

$$k_2^\varepsilon = \varepsilon\bar{k}_2 \quad \Rightarrow \quad \lambda^\varepsilon = \bar{\lambda} = \frac{\bar{k}_2}{\bar{m}_2}\ . \tag{8}$$

so that (6) is rewritten as

$$\varepsilon\bar{m}_1\omega^4 - \left[\varepsilon\bar{\lambda}(\bar{m}_1+\bar{m}_2) - 4\bar{k}_1\varepsilon^{-1}\sin^2(\bar{a}\kappa/2)\right]\omega^2 + 4\bar{\lambda}k_1\varepsilon^{-1}\sin^2(\bar{a}\kappa/2) = 0\ . \tag{9}$$

Although this equation can be analyzed for both long and short waves modes, we are interested in the long one. So, we assume low frequency and bounded wave number, i.e. both ω and κ independent of ε. This option results in the following momentum equation

$$-\omega^2\left[\bar{m}_1+\bar{m}_2-\bar{m}_2\frac{\omega^2}{\omega^2-\bar{\lambda}}\right]u^{(j)} + 4\varepsilon^{-2}\bar{k}_1\sin^2(\frac{\varepsilon\bar{a}}{2}\bar{\kappa})u^{(j)} = \sum_\alpha \bar{f}_\alpha^{(j)} - \frac{\omega^2}{\omega^2-\bar{\lambda}}\bar{f}_2^{(j)}\ . \tag{10}$$

One can pass to the limit $\varepsilon \to 0_+$ in the second term, thus, obtaining the limit momentum equation

$$-\omega^2\left[\bar{m}_1+\bar{m}_2-\bar{m}_2\frac{\omega^2}{\omega^2-\bar{\lambda}}\right]u^{(j)} + \bar{k}_1(\bar{a}\bar{\kappa})^2u^{(j)} = \sum_\alpha \bar{f}_\alpha^{(j)} - \frac{\omega^2}{\omega^2-\bar{\lambda}}\bar{f}_2^{(j)}\ . \tag{11}$$

This model exhibits the dispersive behaviour; $\omega(\kappa)$ is obtained by solving the bi-quadratic equation (see (6))

$$\bar{m}_1\omega^4 - \left[\bar{\lambda}(\bar{m}_1+\bar{m}_2) + k_1(\bar{a}\kappa)^2\right]\omega^2 + \bar{\lambda}\bar{k}_1(\bar{a}\kappa)^2 = 0\ , \tag{12}$$

which yields two dispersion branches and, correspondingly, two phase velocities:

$$\omega_{1,2}^\varepsilon \to \omega_{1,2}^0\ , \quad V_{1,2}^\varepsilon \to V_{1,2}^0\ . \tag{13}$$

There is the *band gap* between the two branches of the dispersion curves, so that for frequencies spanning $]\omega_1^0, \omega_2^0[$ no waves of any wavelength can propagate, see fig. 1(b).

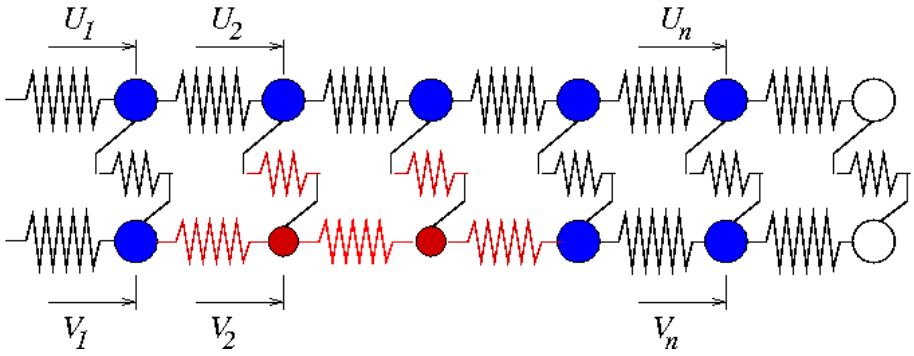

Fig. 2. Scheme of the structure with two interconnected parallel chains; $n = 5$, $n_s = 2$, the *soft substructure* is involved in the lower chain (displacement magnitude V_k).

2.2. Parallel heterogeneous chains

We consider two parallel chains with nonuniform structural parameters (masses and stiffnesses) which vary peridically; the heterogeneous "microstructure" is constituted by periodic distribution of two parallel sub-chains, see Fig. 2. Let each of the substructural chains consist of n nodes (masses) interconnected by springs, j be the substructure index and k be the local mass label relevant to the local substructure, so that the global position x of the mass with labels (j,k) is expressed as $x^{(j,k)} = jL + ka$, where L is the period length and a is the distance between two neighbouring masses in chains. The waves propagating in both the chains are described in terms of the displacement $u^{(j,k)}$ and $v^{(j,k)}$, thus

$$u^{(j,k)} = U_k \exp\{\mathrm{i}\omega t + \mathrm{i}[jL + ka]\kappa\} \ , v^{(j,k)} = V_k \exp\{\mathrm{i}\omega t + \mathrm{i}[jL + ka]\kappa\} \ , \tag{14}$$

The momentum equations written for both chains of the structure (their parameters are labelled with A, B, respectively)

$$\begin{aligned} -\omega^2 m_k^A U_k + k_{k,k+1}^A (U_k - U_{k+1}\exp\{\mathrm{i}a\kappa\}) + k_{k-1,k}^A (U_k - U_{k-1}\exp\{-\mathrm{i}a\kappa\}) + c_k(U_k - V_k) = 0 \ , \\ -\omega^2 m_k^B V_k + k_{k,k+1}^B (V_k - V_{k+1}\exp\{\mathrm{i}a\kappa\}) + k_{k-1,k}^B (V_k - V_{k-1}\exp\{-\mathrm{i}a\kappa\}) + c_k(V_k - U_k) = 0 \ , \end{aligned} \tag{15}$$

where $k_{k,k+1}^A$ is the stiffness of the spring connecting masses m_k^A, m_{k+1}^A and c_k is the stiffness of the "transverse" spring connecting the two chains at position $x^{(j,k)}$. Eq. (15) is supplemented by the periodicity conditions

$$\begin{aligned} U_0 = U_n \ , \quad V_0 = V_n \ , \\ U_{n+1} = U_1 \ , \quad V_{n+1} = V_1 \ . \end{aligned} \tag{16}$$

In analogy with the structure treated above, we shall now pursue the scale dependence of structural parameters, namely dimensions a^ε, $L^\varepsilon = na^\varepsilon$ and spring and mass parameters. We consider sequence of the scale-dependent models (15)-(16). By choosing the modified rescaling of some stiffness parameters we account for soft substructures in each period, so that these substructures will be analogous to disconnected inclusions in solid materials. In particular, we define

$$k_{i,i+1}^{B,\varepsilon} = \begin{cases} \varepsilon \bar{k}_{i,i+1}^B \ , & \text{for } 1 \le i \le n_s + 1 \\ \frac{1}{\varepsilon} \bar{k}_{i,i+1}^B \ , & \text{for } n_s + 2 \le i \le n \end{cases} \qquad c_l^\varepsilon = \begin{cases} \varepsilon \bar{c}_l \ , & \text{for } 2 \le l \le n_s + 1 \ , \\ \frac{1}{\varepsilon} \bar{c}_l \ , & \text{for } l \notin [2, n_s + 1] \ , \end{cases} \tag{17}$$

$$k_{l,l+1}^{A,\varepsilon} = \frac{1}{\varepsilon} \bar{k}_{l,l+1}^A \ , \quad l = 1, \dots, n \ ,$$

whereas all masses are scaled naturally w.r.t. the length, i.e. $m_k^{A,\varepsilon} = \varepsilon \bar{m}_k^A$ and $m_k^{B,\varepsilon} = \varepsilon \bar{m}_k^B$ for $k = 1, \ldots, n$.

Example

We consider $n = 5$ and the soft substructure comprising $n_s = 2$ nodes, labelled by indices $i = 2, 3$, see Fig. 2. The balance of momentum in the substructure reads as

$$\begin{aligned} &-\omega^2 \begin{pmatrix} \bar{m}^B & 0 \\ 0 & \bar{m}^B \end{pmatrix} \begin{bmatrix} V_2 \\ V_3 \end{bmatrix} + \bar{k}^B \begin{pmatrix} 2 & -\exp\{\mathrm{i}a^\varepsilon\kappa\} \\ -\exp\{-\mathrm{i}a^\varepsilon\kappa\} & 2 \end{pmatrix} \begin{bmatrix} V_2 \\ V_3 \end{bmatrix} \\ &-\bar{k}^B \begin{pmatrix} -\exp\{-\mathrm{i}a^\varepsilon\kappa\} & 0 \\ 0 & -\exp\{\mathrm{i}a^\varepsilon\kappa\} \end{pmatrix} \begin{bmatrix} V_1 \\ V_4 \end{bmatrix} + \begin{pmatrix} \bar{c} & 0 \\ 0 & \bar{c} \end{pmatrix} \begin{bmatrix} V_2 - U_2 \\ V_3 - U_3 \end{bmatrix} = \begin{bmatrix} 0 \\ 0 \end{bmatrix} . \end{aligned} \tag{18}$$

Variables V_2, V_3 can be eliminated from the global system on expressing them in terms of V_1, V_4 and U_2, U_3; this can be done on solving the eigenvalue problem

$$\begin{pmatrix} 2\bar{k}^B + \bar{c} & -\bar{k}^B \exp\{\mathrm{i}a^\varepsilon\kappa\} \\ -\bar{k}^B \exp\{-\mathrm{i}a^\varepsilon\kappa\} & 2\bar{k}^B + \bar{c} \end{pmatrix} \begin{bmatrix} w_1^r \\ w_2^r \end{bmatrix} = \lambda^r \bar{m}^B \begin{bmatrix} w_1^r \\ w_2^r \end{bmatrix} , \tag{19}$$

which gives two eigenfrequencies

$$\bar{\omega}^1 = \sqrt{\lambda^1} = \sqrt{\frac{\bar{k}^B + \bar{c}}{\bar{m}}} , \qquad \bar{\omega}^2 = \sqrt{\lambda^2} = \sqrt{\frac{3\bar{k}^B + \bar{c}}{\bar{m}}} . \tag{20}$$

These frequencies bound the region of the *stop band* (band gap). In Fig. 3 we display the dispersion curves for different scales, $\varepsilon \in \{1, 0.5, 0.1, 0.05\}$; For clarity of interpretation of the results we consider $\bar{k}^A_{l,l+1} = 1.5$, $\bar{m}^A_l = 1.5$, $\bar{m}^B_l = 1$ for all $l = 1, \ldots, 5$, $\bar{c}_j = \bar{k}^B_{i,i+1} = 2$ for $j = 2, 3$ and $i = 1, 2, 3$, whereas $\bar{c}_j = \bar{k}^B_{i,i+1} = 1.5$ for all other j, i, i.e. $j \neq 2, 3$ and $i \neq 1, 2, 3$. From these figures it can be deduced, that for different ε small enough (less than 0.1 in our case) the dispersion curves as functions of the measureless wavenumber (in the Brillouin zone) are just rescaled: $\omega_{\varepsilon_2}(\tilde{\kappa}) = \frac{\varepsilon_1}{\varepsilon_2}\omega_{\varepsilon_1}(\tilde{\kappa})$, where $\tilde{\kappa} = \varepsilon\kappa^\varepsilon$. In Fig. 4 we compare the low-frequency dispersion modes revealing existence of the band gap the width of which is ε-independent for ε sufficiently small.

3. Waves in strongly heterogeneous elastic continuum

We consider an elastic medium whose material properties, being attributed to material constituents vary periodically with position; throughout the following text all quantities varying with this microstructural periodicity are denoted with superscript $^\varepsilon$.

The heterogeneous elastic body occupies open bounded domain $\Omega \subset \mathbb{R}^3$, its microstructure is specified by reference cell $Y =]0, 1[^3$ perforated by inclusion $\overline{Y_2} \subset Y$, whereby the matrix part is $Y_1 = Y \setminus \overline{Y_2}$. The decomposition of Ω is generated as follows

$$\begin{aligned} &\Omega_2^\varepsilon = \bigcup_{k \in \mathbb{K}^\varepsilon} \varepsilon(Y_2 + k) \ , \text{ where } \mathbb{K}^\varepsilon = \{k \in \mathbb{Z} |\ \varepsilon(k + \overline{Y_2}) \subset \Omega\} \ , \\ &\Omega_1^\varepsilon = \Omega \setminus \Omega_2^\varepsilon \ . \end{aligned}$$

Properties of the elastic body are described by the standard elasticity tensor c^ε_{ijkl}, where $i, j, k = 1, 2, \ldots, 3$. We assume that inclusions are occupied by a "very soft material" in such a sense that there the material coefficients are significantly smaller than those of the matrix

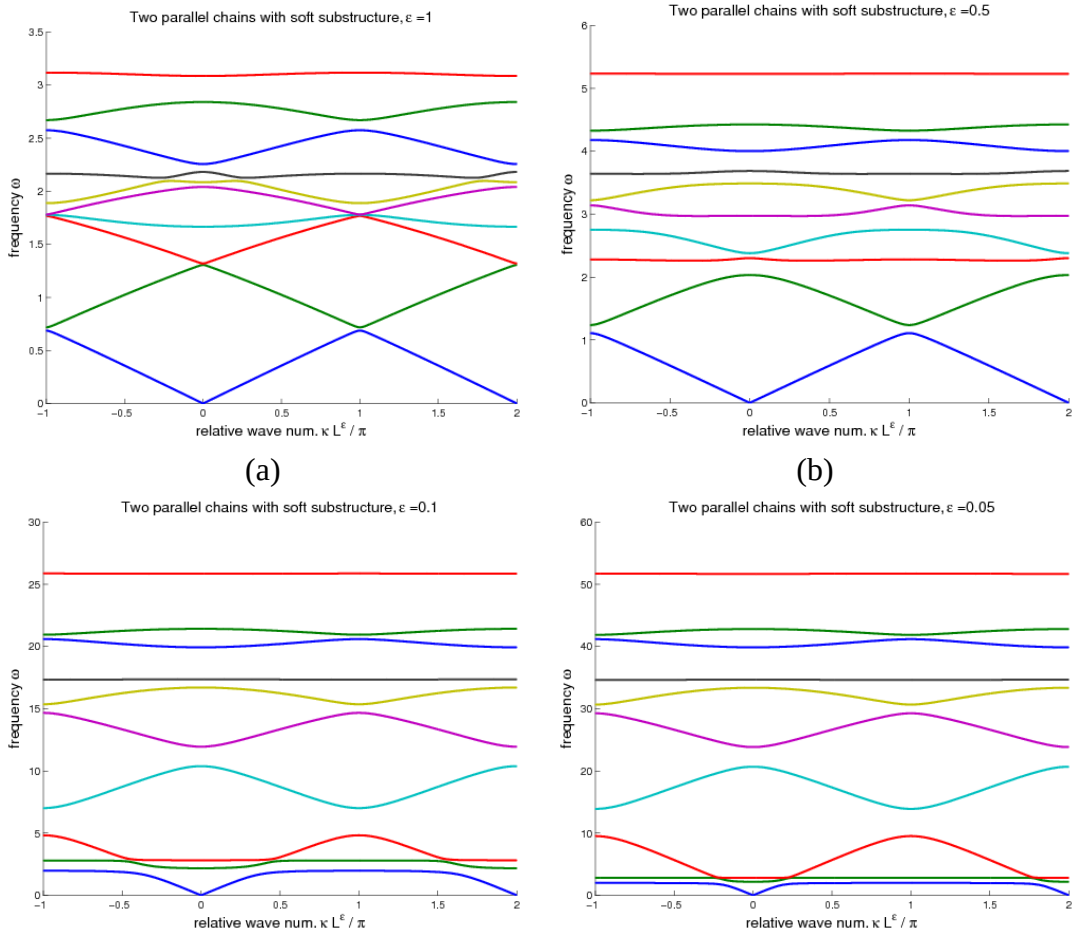

Fig. 3. Dispersion for the 10 node structure for: a) $\varepsilon = 1$, b) $\varepsilon = 0.5$, c) $\varepsilon = 0.1$, d) $\varepsilon = 0.05$.

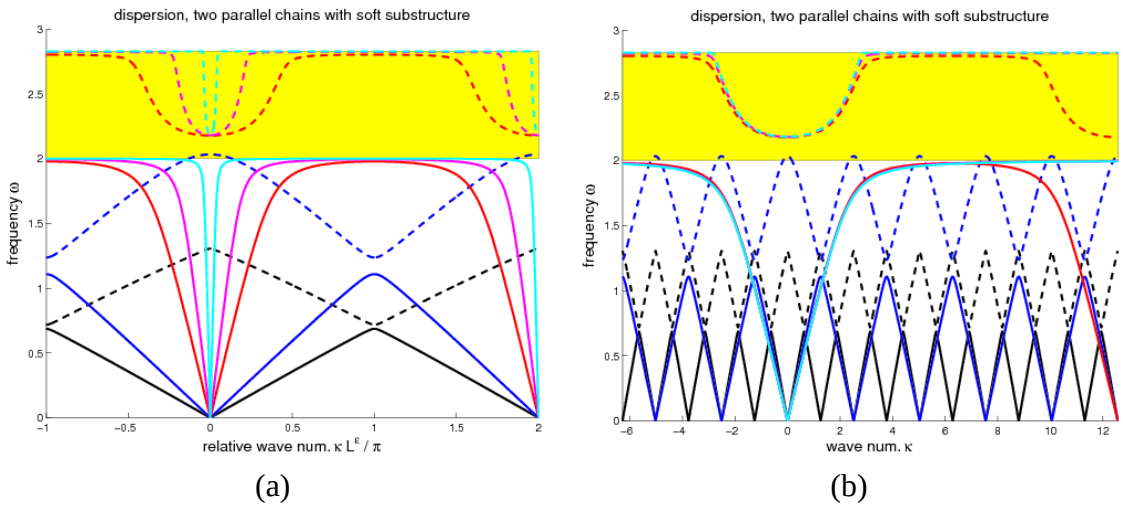

Fig. 4. Dispersion for the 10 node structure. First two modes displayed which are associated with the "soft substructure"; the yellow region bounded by $\bar{\omega}^1, \bar{\omega}^2$ for $\varepsilon \in \{1, 0.5, 0.1, 0.05, 0.01\}$: a) the same relative wave number for all cases, b) fixed range of wave numbers.

compartment, however *the material density* is of the same order of magnitude in both the compartments; as an important feature of the modeling, the *strong heterogeneity* is related to the geometrical scale of the underlying microstructure by coefficient ε^2:

$$\rho^\varepsilon(x) = \begin{cases} \rho^1 & \text{in } \Omega_1^\varepsilon, \\ \rho^2 & \text{in } \Omega_2^\varepsilon, \end{cases} \qquad c^\varepsilon_{ijkl}(x) = \begin{cases} c^1_{ijkl} & \text{in } \Omega_1^\varepsilon, \\ \varepsilon^2 c^2_{ijkl} & \text{in } \Omega_2^\varepsilon. \end{cases}$$

3.1. Problem formulation

We consider stationary wave propagation, assuming a harmonic excitation of a single frequency ω (stationary waves)

$$\tilde{\boldsymbol{f}}(x,t) = \boldsymbol{f}(x)e^{i\omega t} \ ,$$

where $\boldsymbol{f} = (f_i), i = 1,2,3$ is the magnitude field of the applied volumic force. In general, we should expect a dispersive displacement field with magnitude $\boldsymbol{u}^\varepsilon$

$$\tilde{\boldsymbol{u}}^\varepsilon(x,\omega,t) = \boldsymbol{u}^\varepsilon(x,\omega)e^{i\omega t} \ .$$

This allows us to study the steady periodic response of the medium, as characterized by displacement field $\boldsymbol{u}^\varepsilon$ which satisfies the following problem: Find $\boldsymbol{u}^\varepsilon \in \mathbf{H}^1_0(\Omega)$ such that

$$-\omega^2 \int_\Omega \rho^\varepsilon \boldsymbol{u}^\varepsilon \cdot \boldsymbol{v} + \int_\Omega c^\varepsilon_{ijkl} e_{kl}(\boldsymbol{u}^\varepsilon) e_{ij}(\boldsymbol{v}) = \int_\Omega \boldsymbol{f} \cdot \boldsymbol{v} \qquad \forall \boldsymbol{v} \in \mathbf{H}^1_0(\Omega) \ . \tag{21}$$

3.2. Homogenized model

In [3], the unfolding method of homogenization [5] was applied to obtain a limit model when $\varepsilon \to 0$. We just record the resulting system of coupled equations which describe the structure behaviour at two scales, the "macroscopic" one and the "microscopic" one.

First we define the homogenized coefficients involved in the homogenized model of wave propagation. The "frequency–dependent coefficients" are determined just by material properties of the inclusion and by the material density ρ^1, whereas the elasticity coefficients are related exclusively to the matrix compartment.

Frequency–dependent homogenized coefficients involved in the macroscopic momentum equation are expressed in terms of eigenelements $(\lambda^r \boldsymbol{\varphi}^r) \in \mathbb{R} \times \mathbf{H}^1_0(Y_2)$, $r = 1,2,\dots$ of the elastic spectral problem which is imposed in inclusion Y_2 with $\boldsymbol{\varphi}^r = 0$ on ∂Y_2:

$$\int_{Y_2} c^2_{ijkl} e^y_{kl}(\boldsymbol{\varphi}^r)\, e^y_{ij}(\boldsymbol{v}) = \lambda^r \int_{Y_2} \rho^2 \boldsymbol{\varphi}^r \cdot \boldsymbol{v} \quad \forall \boldsymbol{v} \in \mathbf{H}^1_0(Y_2) \ , \quad \int_{Y_2} \rho^2 \boldsymbol{\varphi}^r \cdot \boldsymbol{\varphi}^s = \delta_{rs} \ . \tag{22}$$

To simplify the notation we introduce the *eigenmomentum* $\boldsymbol{m}^r = (m^r_i)$,

$$\boldsymbol{m}^r = \int_{Y_2} \rho^2 \boldsymbol{\varphi}^r .$$

We recover the following tensors, all depending on ω^2:

- Mass tensor $\boldsymbol{M}^* = (M^*_{ij})$

$$M^*_{ij}(\omega^2) = \frac{1}{|Y|}\int_Y \rho \delta_{ij} - \frac{1}{|Y|}\sum_{r\geq 1} \frac{\omega^2}{\omega^2 - \lambda^r} m^r_i m^r_j \ ; \tag{23}$$

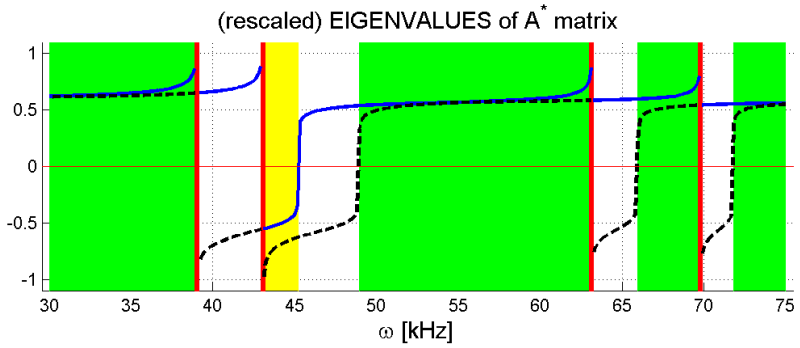

Fig. 5. Low band gap distribution for elliptic inclusion (2D problem). dark grey (green) strips – propagation zone, light grey (yellow) strips – strong band gap, white strips – weak band gaps. As a rule, the strong band gap is always separated from the propagation zone by the "white zones" of the weak band gaps in "anisotropic cases". The curves illustrate eigenvalues of mass tensor $\boldsymbol{M}^*(\omega)$.

- Applied load tensor $\boldsymbol{B}^* = (B^*_{ij})$

$$B^*_{ij}(\omega^2) = \delta_{ij} - \frac{1}{|Y|}\sum_{r\geq 1}\frac{\omega^2}{\omega^2-\lambda^r} m^r_i \int_{Y_2} \boldsymbol{\varphi}^r_j \,. \tag{24}$$

The elasticity coefficients are related to the perforated matrix domain, thus being independent of the inclusions material:

$$C^*_{ijkl} = \frac{1}{|Y|}\int_{Y_1} c_{pqrs} e^y_{rs}(\boldsymbol{w}^{kl} + \boldsymbol{\Pi}^{kl}) e_{pq}(\boldsymbol{w}^{ij} + \boldsymbol{\Pi}^{ij}) \,, \tag{25}$$

where $\boldsymbol{\Pi}^{kl} = (\Pi^{kl}_i) = (y_l \delta_{ik})$ and $\boldsymbol{w}^{kl} \in \mathbf{H}^1_\#(Y_1)$ are the corrector functions satisfying

$$\int_{Y_1} c_{pqrs} e^y_{rs}(\boldsymbol{w}^{kl} + \boldsymbol{\Pi}^{kl}) e^y_{pq}(\boldsymbol{v}) = 0 \quad \forall \boldsymbol{v} \in \mathbf{H}^1_\#(Y_1) \,. \tag{26}$$

The *global equation* – the macromodel – involves the homogenized coefficients. We find $\boldsymbol{u} \in \mathbf{H}^1_0(\Omega)$ such that

$$-\omega^2 \int_\Omega (\boldsymbol{M}^*(\omega^2)\cdot\boldsymbol{u})\cdot\boldsymbol{v} + \int_\Omega C^*_{ijkl} e_{kl}(\boldsymbol{u})\, e_{ij}(\boldsymbol{v}) = \int_\Omega (\boldsymbol{B}^*(\omega^2)\cdot\boldsymbol{f})\cdot\boldsymbol{v} \,, \quad \forall \boldsymbol{v} \in \mathbf{H}^1_0(\Omega) \,. \tag{27}$$

3.3. Band gaps of stationary waves

The acoustic band gaps are frequency intervals of *disabled or restricted* wave propagation. For the homogenized model they are determined by analyzing eigenvalues μ^k of *mass tensor* $M^*_{ij}(\omega)$,

$$\det(M^*_{ij}(\omega) - \mu^k \delta_{ij}) = 0,$$

for any interval spanned by two consecutive eigenvalues, i.e. $\omega \in]\sqrt{\lambda^r}, \sqrt{\lambda^{r+1}}[$. The following band types are distinguished; frequency ω falls into (see Fig. 5):

- strong gap, if all $\mu^k < 0$, so that no wave can propagate;
- weak gap, if there is (k,l): $\mu^k\mu^l < 0$; in this case local wave propagation is confined in the manifold determined by eigenvectors associated with positive eigenvalues;
- propagation zone, if all $\mu^k > 0$, waves of any polarization can propagate.

4. Dispersion of guided waves in periodic media

4.1. Non-homogenized medium

For a finite scale of heterogeneities, guided waves can also be described in terms of the unfolding operator, which allows us to compute the response using the *single reference periodic cell* that represents the periodic structure. We consider

- macroscopic scale x (relevant to global position)
- microscopic scale z (relevant to local position – scale of heterogeneities)

For a given finite scale $\varepsilon > 0$ of heterogeneities we introduce $z = \varepsilon y \in Z := \varepsilon Y$. Using the unfolding operation, the following decomposition is defined

$$x = \bar{x} + \tilde{z} \qquad \text{where } \bar{x}_i = \varepsilon j_i \ , \ j \in \mathbb{Z}^N, \quad x - \bar{x} =: \tilde{z} \in Z \ . \tag{28}$$

Each point in Z oscillates with amplitude $\tilde{\boldsymbol{u}}(\tilde{z})$; the phase shift between different points depends on their mutual distance $\bar{x} + \tilde{z}$, so that

$$\boldsymbol{u} := \tilde{\boldsymbol{u}}(\tilde{z}) \exp\{\mathrm{i}\kappa \cdot (\bar{x} + \tilde{z}) + \mathrm{i}\omega t\}, \tag{29}$$

where $\tilde{\boldsymbol{u}}$ is *Z-periodic*. Accordingly, the strain is computed as $e^x_{ij} = e^{\bar{x}}_{ij} + e^{\tilde{z}}_{ij}$, where

$$\begin{aligned} e_{ij}(\boldsymbol{u}) &= \left[e_{ij}(\tilde{\boldsymbol{u}}) + \frac{1}{2}(\kappa_i \tilde{u}_j + \kappa_j \tilde{u}_i) \right] \exp\{\mathrm{i}\kappa \cdot (\bar{x} + \tilde{z}) + \mathrm{i}\omega t\} \\ &= [e_{ij}(\tilde{\boldsymbol{u}}) + g_{ij}(\tilde{\boldsymbol{u}})] \exp\{\mathrm{i}\kappa \cdot (\bar{x} + \tilde{z}) + \mathrm{i}\omega t\} \ . \end{aligned} \tag{30}$$

Propagation of guided plane waves in periodic medium are analysed using the following spectral problem: Given a *wave vector* $\kappa_i = \varkappa n_i$, $|\boldsymbol{n}| = 1$, find eigenfunctions $\{\boldsymbol{w}^r\}$, $\boldsymbol{w}^r \in \mathbf{H}^1_\#(Z)$ and eigenfrequencies ω^r, $r = 1, 2, \ldots$, such that

$$\begin{aligned} &\int_Z D^\varepsilon_{ijkl} e_{kl}(\boldsymbol{w}^r) e_{ij}(\boldsymbol{v}) + \int_Z D^\varepsilon_{ijkl} g_{kl}(\boldsymbol{w}^r) g_{ij}(\boldsymbol{v}) \\ -\mathrm{i} &\int_Z D^\varepsilon_{ijkl} e_{kl}(\boldsymbol{w}^r) g_{ij}(\boldsymbol{v}) + \mathrm{i} \int_Z D^\varepsilon_{ijkl} g_{kl}(\boldsymbol{w}^r) e_{ij}(\boldsymbol{v}) = (\omega^r)^2 \int_Z \boldsymbol{w} \cdot \boldsymbol{v} \quad \forall \boldsymbol{v} \in \mathbf{H}^1_\#(Z) \ , \end{aligned} \tag{31}$$

where $\boldsymbol{w}^r$ are amplitudes of the eigenmodes and $D^\varepsilon_{ijkl} \equiv c^\varepsilon_{ijkl}$ are the elastic coefficients, defined piecewise in Z.

4.2. Homogenization based analysis

Usually the band gaps are identified from the *dispersion* diagrams. For the homogenized model the dispersion of guided plane waves is analyzed in the standard way, using the following ansatz:

$$\boldsymbol{u}(x,t) = \bar{\boldsymbol{u}}\, e^{-\mathrm{i}(\omega t - x_j \kappa_j)} \ , \tag{32}$$

where $\bar{\boldsymbol{u}}$ is the polarization vector (the wave amplitude) and, again, $\kappa_j = n_j \varkappa$, $|\boldsymbol{n}| = 1$, i.e. $\boldsymbol{n}$ is the incidence direction. The dispersion analysis consists in computing nonlinear dependencies $\bar{\boldsymbol{u}} = \bar{\boldsymbol{u}}(\omega)$ and $\varkappa = \varkappa(\omega)$; for this one substitutes (32) into the homogenized model in its differential Fourier-transformed form

$$-\omega^2 M^*_{ij}(\omega^2) u_j - C^*_{ijkl} \frac{\partial^2 u_k}{\partial x_j \partial x_l} = 0 \ , \text{ thus obtaining} \quad -\omega^2 M^*_{ij}(\omega^2) \bar{u}_j + \varkappa^2\, \Gamma_{ik} \bar{u}_k = 0 \ , \tag{33}$$

where $\Gamma_{ik} = C^*_{ijkl} n_j n_l$ is the Christoffel acoustic tensor. The dispersion is analyzed in terms of the following problem:

- for all $\omega \in [\omega^a, \omega^b]$ and $\omega \notin \{\lambda^r\}_r$ compute eigenelements $(\eta^\beta, \boldsymbol{w}^\beta)$:
$$\omega^2 M^*_{ij}(\omega^2) w^\beta_j = \eta^\beta \Gamma_{ik} w^\beta_k \ , \quad \beta = 1,2,3 \ ; \tag{34}$$
- if $\eta^\beta > 0$, then $\varkappa^\beta = \sqrt{\eta^\beta}$,
- else ω falls in an *acoustic gap*, wave number is not defined.

4.3. Validation of the homogenized model by dispersion analysis

We propose the homogenized model as a tool for estimating the dispersion properties of the heterogeneous solids, however, for this it is necessary to investigate for which *material contrasts* and for which *scales* the homogenized model can be employed. It is important to note, that scale ε determines the ratio between the microstructure size and the wave length; in turn, the homogenization based analysis is relevant for *long waves* only, thereby the whole Brillouin zone can hardly be identified.

We introduce the contrast in elasticity of the two components: $0 < r < 1$, so that (see (28))

$$\begin{aligned} r &= |D^2_{ijkl}|/|\bar{D}^{\mathrm{ref}}_{ijkl}| << 1 \ , \\ D^\varepsilon_{ijkl}(\tilde{z}) &= \begin{cases} D^2_{ijkl} = \varepsilon^2 c^2_{ijkl} = r \bar{D}^{\mathrm{ref}}_{ijkl} & \tilde{z} \in Z_2 \\ D^1_{ijkl} \approx \bar{D}^{\mathrm{ref}}_{ijkl} & \tilde{z} \in Z_1 = Z \setminus Z_2 \ , \end{cases} \end{aligned} \tag{35}$$

where $\bar{D}^{\mathrm{ref}}_{ijkl}$ is the reference elasticity tensor. Hence, given $\varepsilon > 0$ we obtain $c^2_{ijkl} = D^2_{ijkl}/\varepsilon^2 = D^{\mathrm{ref}}_{ijkl}\ r/\varepsilon^2$ and we can compute eigenfrequencies $\lambda^k_{(r,\varepsilon)}$ defined by (22) where the clamped inclusion is $Y_2 = \frac{1}{\varepsilon} Z_2$. Alternatively, we may introduce "reference eigenvalues" $\bar{\lambda}^k$ defined also by (22), however with the elasticity therein replaced by $\bar{D}^{\mathrm{ref}}_{ijkl}$. Thus, for any combination (r,ε) of the contrast and scale the "rescaled eigenvalues" are

$$\lambda^k_{(r,\varepsilon)} = \frac{r}{\varepsilon^2} \bar{\lambda}^k \ , \quad k = 1,2,\dots \ ,$$

these are used to compute the actual mass matrix $\boldsymbol{M}^{*(r,\varepsilon)}$ by (23). Consequently, for (r,ε) we can compare the dispersion response computed for the heterogeneous model (31) or for the homogenized one (34):

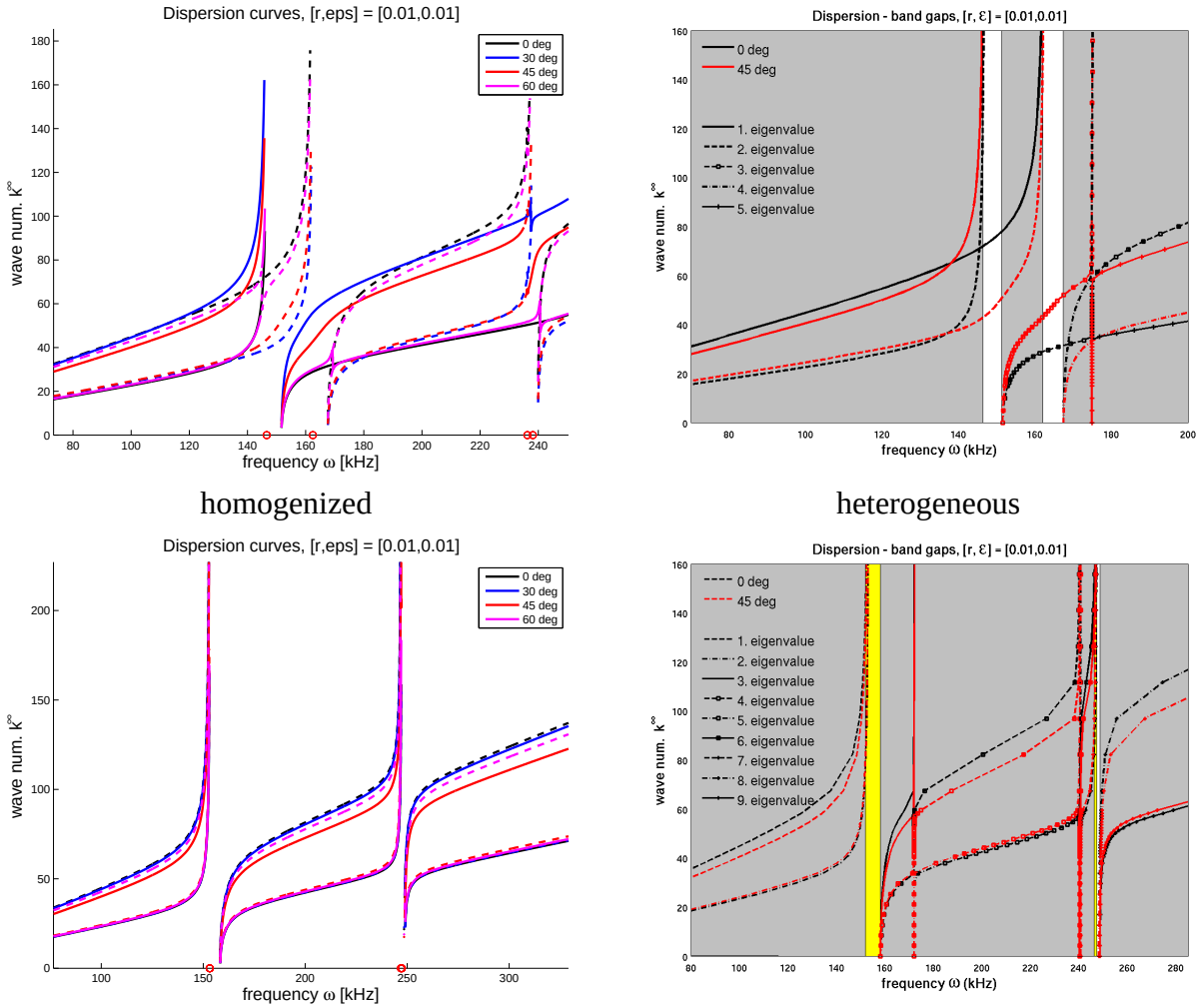

Fig. 6. Dispersion curves $\varkappa - \omega$ for the homogenized model (left) and for the FE heterogeneous model (right); above: *elliptic* inclusions, below: *circular* inclusions; contrast and scale parameters: $r = 0.01$ and $\varepsilon = 0.01$. In the right-hand-side figures the weak and strong band gaps, as indicated by white and yellow (grey) strips, respectively, were computed by the homogenized model for stationary waves. The strong band gaps *do not appear* in the "anisotropic case", as here represented by the elliptic geometry.

- *Heterogeneous model* (31). Given $\varkappa \in]0, \overline{\varkappa}[$, compute frequencies $\{\omega^k(\varkappa)\}_k$, where $k = 1, 2, \ldots, \overline{k}$; assuming $\omega^k \leq \omega^{k+1}$, only low modes ($\overline{k}$ small) is needed, since we are interested in low band gaps.
- *Homogenized corrected model* (34). Given a (low) frequency range $\omega \in]\underline{\omega}, \overline{\omega}[\setminus \{\lambda^k_{(r,\varepsilon)}\}_k$ (resonance modes excluded), compute wave numbers $\{\varkappa^\beta(\omega)\}$, $\beta = 1, 2, 3$ (for 3D problems).

According to our observations, when $r = 0.01$ (larger contrast), the homogenization based approximation is accurate sufficiently, as demonstrated in Fig. 6.

5. Conclusion

This study has proved a great potential in modeling phononic materials (crystals) using the homogenization approach which was elaborated rigorously in [3] by the unfolding method of

homogenization [5, 6], although a formal treatment by the asymptotic expansion was discussed much earlier in [1]. Here we focused on some practical aspects of the model applicability to real structures with a given material composition. The homogenized model, which must be corrected for given material contrast and geometrical scale, serves as an easy-to-use computational tool for an approximate prediction of the low band gap distribution. Thus, it can be very interesting to follow this approach in development of optimum designed phononic materials, see [7]. Recently the model has been extended to the piezo-phononic materials [8, 9] featured by coupling strain and electric field.

Acknowledgements

This work has been supported by the projects MSM 1M06031 and GACR 101/07/1471 of the Czech Republic.

References

[1] J.L. Auriault, G. Bonnet, Dynamique des composites elastiques periodiques, Arch. Mech., 37 (1985), 269-284.

[2] A. Ávila, G. Griso, B. Miara, Bandes phononiques interdites en élasticité linéarisée, C. R. Acad. Sci. Paris, Ser. I 340, 2005, 933-938.

[3] A. Ávila, G. Griso, B. Miara, E. Rohan, Multi-scale modelling of elastic waves – theoretical justification and numerical simulation of band gaps, Accepted for publication in MMS, SIAM, (2007).

[4] G. Bouchitté, D. Felbacq, Homogenization near resonances and artificial magnetism from dielectrics, C. R. Acad. Sci. Paris, Ser. I 339, (2004) 377-382.

[5] A. Cioranescu, A. Damlamian, G. Griso, Periodic unfolding and homogenization. C. R. Acad. Sci. Paris, Ser. I 335 (2002) 99-104.

[6] A. Damlamian, An elementary introduction to Periodic Unfolding. GAKUTO International series Math. Sci. Appl. Vol. 24, (2005) Multi scale problems and Asymptotic Analysis, 119-136.

[7] E. Rohan, B. Miara, Modelling and sensitivity analysis for design of phononic crystals. PAMM, Proc. Appl. Math. Mech. 6, (2006) 505-506.

[8] E. Rohan, B. Miara, Sensitivity analysis of acoustic wave propagation in strongly heterogeneous piezoelectric composite. In: Topics on Mathematics for Smart Systems, World Sci. Publ., (2006) 139-207.

[9] E. Rohan, B. Miara, Homogenization and shape sensitivity of microstructures for design of piezoelectric bio-materials, Mechanics of Advanced Materials and Structures 13 (2006) 473-485.

[10] E. Yablonovitch, Photonic band-gap crystals. J. Phys. Condens. Matter, 5, (1993) 2443-2460.